P H Y S I C A L   R E V I E W   L E T T E R S

# Rydberg Atom Formation in Ultracold Plasmas:
# Small Energy Transfer with Large Consequences

T. Pohl,[1] D. Vrinceanu,[2] and H. R. Sadeghpour[1]

[1]*ITAMP, Harvard-Smithsonian Center for Astrophysics, 60 Garden Street, Cambridge, Massachusetts 02138, USA*
[2]*Theoretical Division, Los Alamos National Laboratory, Los Alamos, New Mexico 87545, USA*

We present extensive Monte Carlo calculations of electron-impact-induced transitions between highly excited Rydberg states and provide accurate rate coefficients. For moderate energy changes, our calculations confirm the widely applied expressions in P. Mansbach and J. Keck [Phys. Rev. **181**, 275 (1969)] but reveal strong deviations at small energy transfer. Simulations of ultracold plasmas demonstrate that these corrections significantly impact the short-time dynamics of three-body Rydberg atom formation. The improved rate coefficients yield quantitative agreement with recent ultracold plasma experiments.

The advent of ultracold plasmas [1], the realization of cold Rydberg gases [2], and the production of highly excited cold antihydrogen atoms [3,4] have focused attention on the multitude of collisional and radiative processes that occur in ionized gases. At low temperatures, Rydberg atom formation is dominated by collisional three-body recombination (TBR). The subsequent evolution of Rydberg state population is predominantly driven by electron-impact excitation, deexcitation, and ionization. A detailed knowledge of the corresponding transition rates is essential for understanding the dynamics of plasmas, ranging from laser-produced nanoplasmas [5–7] to cold glow discharges [8] and various astrophysical and early Universe plasmas [9–13].

In an early seminal work, Mansbach and Keck (MK) [14] performed classical calculations of electron-impact deexcitation of Rydberg states, from which the complete set of collision rates for (de)excitation, ionization, and TBR has been inferred [14,15]. The corresponding fit formulas for the rate coefficients have been widely applied during the past four decades and provide a foundation for the interpretation of current ultracold neutral plasma (UNP) experiments [16–22].

Here we perform accurate Monte Carlo (MC) trajectory calculations of collisional rate coefficients that reveal substantial deviations from the MK results [14] (Fig. 1). We demonstrate the significance of the rate corrections with simulations of the recent UNP experiments by Fletcher *et al.* [21], in which short-time Rydberg atom formation in an expanding UNP was monitored. Figure 2 shows that the MK rates noticeably overestimate the observed TBR rate, while the present rate coefficients yield a much improved description of the observed recombination dynamics.

Complementary to the variational reaction rate approach of Ref. [14], we performed direct classical MC trajectory calculations of electron collision-induced transition rates.

While this method is commonly used to obtain collisional cross sections [23], we employ it here to directly evaluate the differential rates for energy change from $\varepsilon_i$ to $\varepsilon_f$ according to

$$\frac{dk(\varepsilon_i, \varepsilon_f; T)}{d\varepsilon_f} = \frac{2\pi b_0}{N\Delta\varepsilon} \sum_{j=1}^{N} \theta(\epsilon_j, \varepsilon_f, \Delta\varepsilon) b_j v_j e^{b_j/b_0}, \quad (1)$$

where $N$ is the total number of trajectories. The summation includes only trajectories which have a final temperature-scaled energy $\varepsilon_j$ within a range $\Delta\varepsilon$ around $\varepsilon_f$. This is expressed by the step function $\theta$, which is unity for $|\epsilon_j - \varepsilon_f| < \Delta\varepsilon/2$ and zero otherwise. Initially, the target is selected from a microcanonical distribution of states with binding energy $\varepsilon_i$, the impact parameters $b_j$ are sampled from an exponential distribution $\propto e^{-b_j/b_0}$, and the velocities $v_j$ have a Maxwellian distribution with temperature $T$.
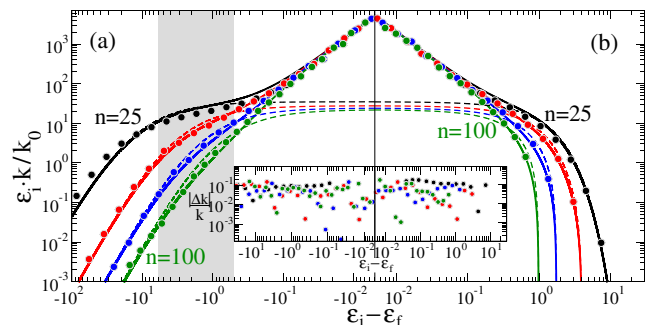


FIG. 1 (color online).   (a) Deexcitation and (b) excitation rate coefficients for different values of the initial energy $\varepsilon_i$, in increments of $\Delta n_i = 25$ at $T = 16$ K. The MC data (symbols) are nicely fitted by the improved expressions Eqs. (2) (solid lines) and deviate from the MK results (dashed lines) for small $\Delta\varepsilon$. The shaded area marks the energy range investigated in Ref. [14], where both rate formulas agree. The inset shows the relative deviation $|\Delta k/k|$ of the numerical data from Eq. (2).
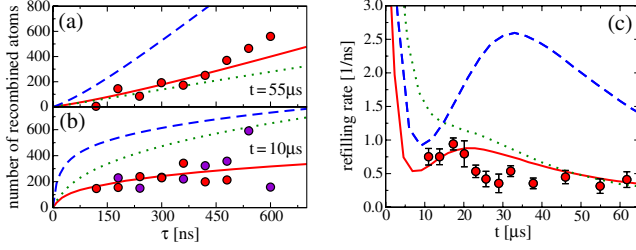
223201-1

FIG. 2 (color online). (a),(b) Actual number of recombined atoms and (c) Rydberg atom refilling rate, as measured in Refs. [21,37]. Compared to the predictions of the MK rates (dashed lines) and the VS rates (dotted lines), plasma simulations based on the present rates (solid lines) yield an improved description of the experimental data (dots). The experimental data points at $t = 10$ $\mu$s include two separate measurements.

The parameter $b_0$ is chosen sufficiently large to ensure convergence of the calculated rates.

Compared to the standard impact parameter sampling, the exponential importance sampling yields considerably improved convergence, allowing us to calculate transition rates over a wide range of initial energies ($25 \leq n_i \leq 200$) and temperatures ($4$ K $\leq T \leq 256$ K). This corresponds to $0.02 \leq \varepsilon_i \leq 63$ and is achieved by running a total of $6 \times 10^6$ trajectories. Figures 1 and 3 illustrate our results, accurately described by the improved rate formulas

$$k(n_i, n_f) = k_0 \frac{\varepsilon_i^{5/2} \varepsilon_f^{3/2}}{\varepsilon_>^{5/2}} e^{-(\varepsilon_i - \varepsilon_<)} \left[ \frac{22}{(\varepsilon_> + 0.9)^{7/3}} \right.$$
$$\left. + \frac{9/2}{\varepsilon_>^{5/2} \Delta\varepsilon^{4/3}} \right], \qquad (2)$$

$$k_{\mathrm{ion}}(n_i) = \frac{k_{\mathrm{tbr}}(n_i)}{n_i^2 \Lambda^3 \rho_e e^{\varepsilon_i}} = \frac{11(\mathcal{R}/k_B T)^{1/2} k_0 e^{-\varepsilon_i}}{\varepsilon_i^{7/3} + 4.38\varepsilon_i^{1.72} + 1.32\varepsilon_i}, \quad (3)$$

where $k_0 = e^4/(k_B T \sqrt{m\mathcal{R}})$, $\varepsilon_{i(f)} = \mathcal{R}/n_{i(f)}^2 k_B T$, $\Delta\varepsilon = |\varepsilon_f - \varepsilon_i|$, $\varepsilon_< = \min(\varepsilon_i, \varepsilon_f)$, $\varepsilon_> = \max(\varepsilon_i, \varepsilon_f)$, $\mathcal{R} \approx$
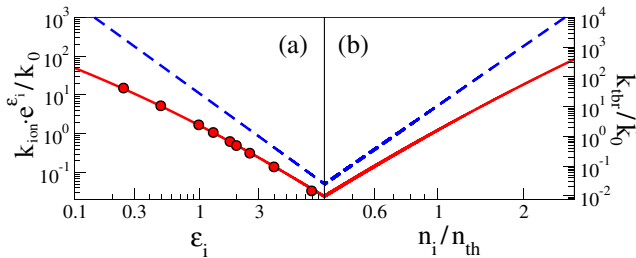


FIG. 3 (color online). (a) Ionization and (b) recombination rate coefficients for different values of the initial energy $\varepsilon_i$. The MC data (symbols) are well described by Eq. (3) (solid lines) but are significantly smaller than the MK rates (dashed lines). $n_{\mathrm{th}} = \sqrt{\mathcal{R}/k_B T}$ and $\tilde{k}_0 = n_{\mathrm{th}}^3 \Lambda^3 \rho_e k_0$.

13.6 eV is the Rydberg constant, $\Lambda = \sqrt{h^2/2\pi m k_B T}$ is the thermal de Broglie wavelength, $\rho_e$ and $m$ are the electron density and mass, respectively, and $k_B$ is the Boltzmann constant.

The comparison of the numerical data to Eq. (2) and the MK expression [14] demonstrates the quality of our fit formulas. The MK rate coefficients were deduced solely from calculated deexcitation rates for $0.5 \leq \Delta\varepsilon \leq 6$ and $1 \leq \varepsilon_f \leq 10$. In this regime, Eqs. (2) and (3) approach the MK expressions. Our calculations extend this energy range to $0.2 \leq \varepsilon_f \leq 250$ and $10^{-3} \leq \Delta\varepsilon \leq 100$.

While our covered energy range does not allow us to accurately fit the large-$\Delta\varepsilon$ regime, the plasma dynamics discussed in this work is not affected by this deviation, since the total rates are extremely small for large $\Delta\varepsilon$. Recent experiments and calculations [24,25], however, have identified such large energy transfer collisions as a mechanism for forming deeply bound antihydrogen atoms. Indeed, both experimental and theoretical field ionization spectra were found to be consistent with an asymptotic deexcitation rate scaling of $k \propto \varepsilon_f^{-3.33}$, suggesting that the predicted power-law decay persists at large $\varepsilon_>$.

For small energy transfer, however, the MK expressions quantitatively differ from the present results and miss the singular behavior with decreasing $\Delta\varepsilon$. This diverging $\Delta\varepsilon$ dependence also appears in previous—approximate—calculations (see, e.g., [26,27]), whose predicted exponent is, however, inconsistent with our MC data. Our directly determined ionization rate [Eq. (3)] significantly differs from this expression but agrees with the semiempirical formula of Vriens and Smeets (VS) [27] [Fig. 3(a)]. Consequently, there is a substantial difference in the rate for recombination. In contrast to the $n^{6.66}$ scaling of the MK TBR rate, Eq. (3) yields a weaker $n^4$ dependence and, hence, a much smaller initial formation rate of Rydberg atoms.

Having established expressions for the full set of rate coefficients, we can examine consequences for the plasma evolution. Following [28], we determine the steady-state distribution of Rydberg levels in a recombining plasma, by adiabatically eliminating the dynamics of excited state populations. Figure 4 shows the calculated level populations $\xi(n)$, normalized to the corresponding equilibrium Saha distribution [28]. Both sets of rate coefficients yield similar distributions. In particular, the kinetic bottleneck—marked by the sudden drop of $\xi(n)$ [15]—in both cases appears at $\sim 4k_B T$. In fact, a calculation of the collisional, steady-state recombination rate $\alpha$ yields the familiar temperature scaling

$$\alpha = C_{\mathrm{rec}} T^{-9/2}, \qquad (4)$$

with a coefficient $C_{\mathrm{rec}} = 2.77 \times 10^{-9}$ K$^{9/2}$ cm$^6$ s$^{-1}$, 30% smaller than the value obtained by MK [14].

While steady-state quantities are weakly affected by the present rate corrections, the availability of accurate
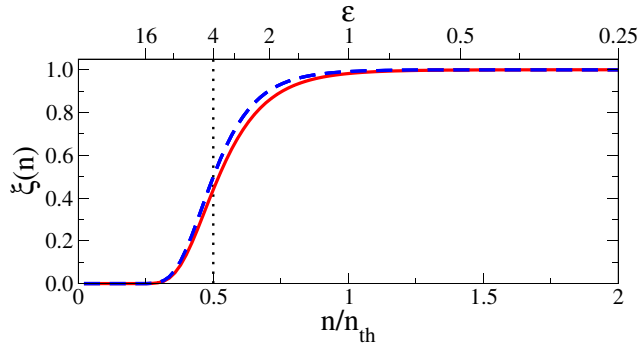
FIG. 4 (color online).   Normalized steady-state Rydberg population in a recombining plasma, obtained from the MK rates (dashed line) and the new coefficients in Eqs. (2) and (3) (solid line). The vertical dotted line marks the bottleneck energy of $4k_BT$.
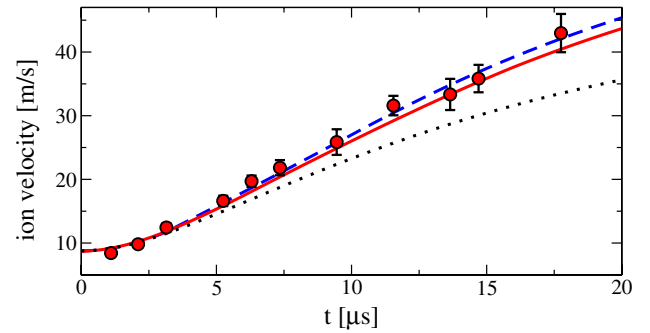


FIG. 5 (color online).   Measured [20] expansion velocity of an ultracold strontium plasma (dots) compared to simulations using the present rate coefficients in Eqs. (2) and (3) (solid line) and the MK rate coefficients (dashed line). The dotted line shows the resulting expansion dynamics when recombination is neglected.

collision rates is crucial for describing the formation of Rydberg states under nonequilibrium conditions. Whereas a direct experimental probe of recombination is complicated in conventional and astrophysical plasmas, UNPs, on the other hand, with their high degree of initial state control, offer a clean venue to study recombination. Driven by the thermal electron pressure, the plasma subsequently expands into vacuum on a microsecond time scale [29,30]. Recombination causes considerable electron heating [20] and, hence, affects the expansion of the plasma.

A quantitative discussion of these experiments, hence, requires a consistent treatment of the entire plasma evolution, describing the interplay between expansion, disorder-induced heating, and Rydberg atom formation [31]. We account for these processes by performing UNP simulations, similar to those of Refs. [20,31]. Briefly, we employ an adiabatic description of the electron component, based on the electronic nonideal equation of state, and a direct particle-in-cell propagation of the ions, which is coupled to a MC treatment of TBR and electron-Rydberg atom collision. A noteworthy improvement compared to previous approaches is that we relax the assumption of a common, but *ad hoc*, cutoff at $\varepsilon = 1$ [18,19,32]. Instead, the high-$n$ divergence of the recombination rate is systematically removed by including ionization [33] due to low-frequency ionic microfields [34,35].

Recently, absorption imaging of strontium ions was employed to accurately monitor the time evolution of the ion expansion velocity [20]. Detailed comparison with simulations revealed substantial heating due to recombination, which was successfully described by using the MK collision rates. Indeed, our simulations show that both the MK and the present transition rates yield similar expansion dynamics in agreement with the experiment (see Fig. 5). This behavior can be understood from well-separated time scales for expansion of the plasma and relaxation of highly excited Rydberg states towards local thermodynamic equi-

librium (LTE). The initial acceleration of plasma ions normally takes up to several microseconds before the onset of considerable expansion, providing sufficient time to develop a LTE of high-Rydberg state populations. As we have shown above, the latter depends only weakly on the details of the individual collision rates, which explains their rather modest effect on the expansion velocity. The differences in the rate coefficients, however, are more pronounced in non-LTE situations, as also occurring in an astrophysical context (see, e.g., [12]).

Nonequilibrium, short-time dynamics of Rydberg atom formation was recently monitored for the first time in UNPs, by applying a sequence of two microwave pulses to an ultracold xenon plasma [21]. A first $\sim 100$ ns pulse, applied at time $t$, ionized atoms above $n = 35$. After a time delay $\tau$, a second identical pulse was employed to measure the number of recombined Rydberg atoms. By varying both the time $t$ and the delay $\tau$, this scheme allows us to monitor the short-time formation of Rydberg atoms [Figs. 2(a) and 2(b)] and the time evolution of the Rydberg refilling rate [Fig. 2(c)] during the plasma expansion.

One peculiarity in describing the experiment lies in an appropriate description of the Rydberg atom ionization, which results from the combined action of the external microwave field and fluctuating electric fields caused by the surrounding plasma ions. If the value $F_{mf}$ of the local ionic microfield exceeds the minimum microwave field ionization threshold $F_n = 1/(3n^5)$ a.u. [36], fast Stark mixing of highly excited states leads to rapid ionization. This prevents electrons liberated in ionization of atoms with $n > (3F_{mf})^{1/5}$ from gaining sufficient energy to leave the plasma to be detected. Since our simulations already determine the evolving distribution of plasma microfields, this effect is incorporated by weighting the atomic level population with an effective occupation probability, as introduced in Ref. [34].

In Fig. 2, we compare the experimental results to our plasma simulations, utilizing the MK (dashed lines) and

the VS (dotted lines) as well as the present (solid lines) rate coefficients. The actual number of recombined atoms and the corresponding Rydberg atom refilling rates are over-estimated using the MK rate coefficients. While at longer times the VS rates yield a recombination dynamics similar to that predicted by Eqs. (2) and (3) [Fig. 2(a)], they reveal significant differences as compared to our results and the experiment [Fig. 2(b)]. This is due to a larger electron density at earlier times in the plasma expansion, giving rise to more electron-Rydberg scattering events, whose rate coefficients are different in our MC calculations and in the VS semiempirical rates.

The theoretical curves are obtained from full simulations of the long-time plasma dynamics up to time $t$ followed by the Rydberg atom refilling phase in between the two pulses. A previous analysis used the steady-state recombi-nation rate coefficient $\alpha$ to extract electron temperatures from the measured Rydberg atom formation rates [21]. The resulting temperature evolution was found to be in good agreement with simulations based on the MK rates. This can be attributed to the insensitivity of the long-time plasma evolution to the present rate corrections (Fig. 5) and to the strong temperature dependence of $\alpha$ [Eq. (4)], making the extracted temperatures only weakly dependent on the precise value of the coefficient $C_{\mathrm{rec}}$. On the other hand, Fig. 2 demonstrates that the refilling rate is a sensi-tive probe of the recombination dynamics and provides a clear propensity for the current rate improvements.

In summary, we have reported exhaustive Monte Carlo calculations of Rydberg atom formation, electron collision-induced excitation, deexcitation, and ionization and employed the resulting rate coefficients in particle-in-cell simulations of ultracold plasma evolution. It emerges that a modification of widely applied rate coefficients is necessary for quantitative description of the short-time recombination dynamics, as measured recently by micro-wave ionization in an ultracold plasma [21]. As highlighted here, UNP experiments may offer the distinct opportunity to quantitatively assess various collisional processes occur-ring in plasmas and to illuminate the details of Rydberg atom formation.

[1] T. C. Killian *et al.*, Phys. Rev. Lett. **83**, 4776 (1999).
[2] M. P. Robinson *et al.*, Phys. Rev. Lett. **85**, 4466 (2000).
[3] M. Amoretti *et al.*, Nature (London) **419**, 456 (2002).
[4] G. Gabrielse *et al.*, Phys. Rev. Lett. **89**, 213401 (2002).
[5] H. Wabnitz *et al.*, Nature (London) **420**, 482 (2002).
[6] C. Jungreuthmayer *et al.*, J. Phys. B **38**, 3029 (2005).
[7] U. Saalmann *et al.*, J. Phys. B **39**, R39 (2006).
[8] G. G. Lister, Phys. Plasmas **10**, 2136 (2003).
[9] J. W. Ferguson and G. J. Ferland, Astrophys. J. **479**, 363 (1997).
[10] K. R. Anantharamaiah *et al.*, Nature (London) **315**, 647 (1985).
[11] S. V. Stepkin *et al.*, Mon. Not. R. Astron. Soc. **374**, 852 (2007).
[12] P. S. Barklem, Astron. Astrophys. **466**, 327 (2007).
[13] M. Piembert *et al.*, Astrophys. J. **666**, 636 (2007).
[14] P. Mansbach and J. Keck, Phys. Rev. **181**, 275 (1969).
[15] J. Stevefelt *et al.*, Phys. Rev. A **12**, 1246 (1975).
[16] T. Topcu *et al.*, Phys. Rev. A **74**, 062708 (2006).
[17] T. C. Killian *et al.*, Phys. Rev. Lett. **86**, 3759 (2001).
[18] F. Robicheaux and J. D. Hanson, Phys. Rev. Lett. **88**, 055002 (2002).
[19] T. Pohl *et al.*, Phys. Rev. A **70**, 033416 (2004).
[20] P. Gupta *et al.*, Phys. Rev. Lett. **99**, 075005 (2007).
[21] R. S. Fletcher *et al.*, Phys. Rev. Lett. **99**, 145001 (2007).
[22] S. D. Bergeson and F. Robicheaux, arXiv:0708.2922.
[23] D. Vrinceanu, Phys. Rev. A **72**, 022722 (2005).
[24] T. Pohl *et al.*, Phys. Rev. Lett. **97**, 143401 (2006).
[25] G. Gabrielse, Adv. At. Mol. Opt. Phys. **50**, 155 (2005).
[26] M. Gryziński, Phys. Rev. **115**, 374 (1959).
[27] L. Vriens and A. H. M. Smeets, Phys. Rev. A **22**, 940 (1980).
[28] D. R. Bates *et al.*, Proc. R. Soc. A **267**, 297 (1962).
[29] S. Kulin *et al.*, Phys. Rev. Lett. **85**, 318 (2000).
[30] S. Laha *et al.*, Phys. Rev. Lett. **99**, 155001 (2007).
[31] T. C. Killian *et al.*, Phys. Rep. **449**, 77 (2007).
[32] Y. Hahn, Phys. Lett. A **231**, 82 (1997).
[33] M. J. Rakovic and S. I. Chu, J. Phys. B **31**, 1989 (1998).
[34] D. G. Hummer and D. Mihalas, Astrophys. J. **331**, 794 (1988).
[35] A. Y. Potekhin *et al.*, Phys. Rev. E **65**, 036412 (2002).
[36] T. F. Gallagher, *Rydberg Atoms* (Cambridge University Press, Cambridge, England, 1994).
[37] R. S. Fletcher, X. L. Zhang, and S. L. Rolston (private communication).